Available online at www.sciencedirect.com
ScienceDirect
Experimental Thermal and Fluid Science 32 (2008) 1279–1286
Experimental Thermal and Fluid Science
www.elsevier.com/locate/etfs

The local heat transfer mathematical model between vibrated fluidized beds and horizontal tubes

Zhu Xuejun [a,b], Ye Shichao [a,*], Pan Xiaoheng [a]

[a] School of Chemical Engineering, Sichuan University, Chengdu 610065, PR China
[b] College of Biology and Chemical Engineering, Panzhihua University, Panzhihua 617000, PR China

Received 30 September 2007; received in revised form 22 February 2008; accepted 22 February 2008

Abstract

A dimensionless mathematical model is proposed to predict the local heat transfer coefficients between vibrated fluidized beds and immersed horizontal tubes, and the effects of the thickness of gas film and the contact time of particle packets are well considered. Experiments using the glass beads (the average diameter $\bar{d}_p = 1.83$ mm) were conducted in a two-dimensional vibrated fluidized bed (240 mm × 80 mm). The local heat transfer law between vibrated fluidized bed and horizontal tube surface has been investigated. The results show that the values of theoretical prediction are in good agreement with experimental data, so the model is able to predict the local heat transfer coefficients between vibrated fluidized beds and immersed horizontal tubes reasonably well, and the error is in range of ±15%. The results can provide references for future designing and researching on the vibrated fluidized beds with immersed horizontal tubes.

Keywords: Vibrated fluidized bed; The local heat transfer coefficient; Immersed horizontal tube; Mathematical model

1. Introduction

There exist high heat transfer rate of fluidized beds and immersed surface, and little temperature variation across the bed, and can be obtained higher heat transfer coefficients compared to a conventional fluidized beds [1]. Due to these advantages, this technology has been applied commercially in various processes, such as fluidized bed combustor [2], fluidized bed reactor [3], fluidized bed dryer, [4], etc.

Several models have been proposed for predicting the local heat transfer coefficients between fluidized beds and immersed surface. (1) *Film model*. Dow and Jakob [5] proposed a gas film model. Bed particles were treated as obstacles to reduce resistance by scouring away the film. This hypothesis is not supported by the experiments results [6,7]. (2) *Packet model*. This model first proposed by Mickley and Fairbanks [8]. It works reasonably in which residence time of packets is long or the particle diameter is small [9]. But the error is likely to be significant for short contact time. Several modifications were made to improve the packet model, but all the models are restricted in application to the particle sizes less than 0.5 mm [10]. (3) Particle model. This model was based on unsteady conduction to the particles and the heat transfers from distinct particles rather than particle packets [11]. This type of model includes the single-particle model, two-particle model, four-particle model, etc., [12]. Particle model must be brought in gas film between the surface and the first row of particles to obtain good data fitness. Heat transfer in fluidized beds with horizontal tubes has been experimentally investigated by many researchers [13,14]. Many empirical correlations for predicting the local heat transfer coefficients were established from experimental results [15]. While their models and experiments did not consider the vibration, and a large amount of experimental data were obtained with small particle diameter ($\bar{d}_p < 1$ mm). There

* Corresponding author. Tel.: +86 28 6630 3232; fax: +86 28 8540 1819.
E-mail address: zxjpzh@tom.com (S.C. Ye).

0894-1777/$ - see front matter © 2008 Elsevier Inc. All rights reserved.
doi:10.1016/j.expthermflusci.2008.02.007

Nomenclature

a,b,c	coefficient of Eq. (15), dimensionless
Ar	Archimedes number $(=d_p^3\rho_f(\rho_s-\rho_f)g/\mu_f^2)$, dimensionless
A_i	local heat transfer area, m^2
Bi	Biot number, dimensionless
c_p	heat capacity, J kg^{-1} K^{-1}
d_p	particle diameter, mm
D_b	bubble diameter, mm
D_t	tube diameter, mm
f	vibration frequency, Hz
f_0	fraction of bubble, dimensionless
Fo	Fourier number, dimensionless
H_0	height of the bed, mm
h_{gc}	particle convective heat transfer coefficient, W m^{-2} K^{-1}
h_i	local heat transfer coefficient, W m^{-2} K^{-1}
k	thermal conductivity, W m^{-1} K^{-1}
N	fluidization number, $(N=u/u_{mf})$
Pr	Prandtl number, dimensionless
Re	Reynolds number, dimensionless
t	time, s
T_b	bed temperature, °C
T_{b0}	bed temperature at $x=0$, °C
$T_{b\infty}$	bed temperature at $x=$ infinity, °C
T_w	temperature of the tube surface, °C
u	gas velocity, m s^{-1}
x	coordinate
v	direction of vibration

Greek symbols

α	thermal diffusivity, m^2 s^{-1}
ε_0	bed void fraction, m^3 m^{-3}
Γ	vibration strength $(=A(2\pi f)^2/g)$, dimensionless
μ_f	gas viscosity, Pa s
ρ	density, kg m^{-3}
ρ_b	accumulate density, kg m^{-3}
θ	angular position on the tube surface, degree

Subscripts

e	particle-packet
g	gas
p	particle
mf	critical fluidization state with conventional fluidized bed
mfv	critical fluidization state with vibrated fluidized bed

were relatively fewer studies for the local heat transfer coefficients of large particles between vibrated fluidized bed and immersed horizontal tubes. The hydrodynamic behavior of small particles can be different from those of large particles, and the correlations obtained from small particles can not be used to large particles. The gas convective can be ignored for small particles, but becomes important when the particle diameter is larger than 1 mm [16]. The mechanical vibration imposed on fluidized beds can significantly improve the gas–solid contact and the fluidization behavior, strengthen the heat and mass transfer, and break the bubbles more efficiently [17], and can also be decreased the critical fluidization velocity [18], affect the gas film thickness around the tube surface.

It is important to understand the heat transfer mechanism to predict the local heat transfer coefficients between vibrated fluidized beds and horizontal tubes precisely. In this study, the dimensionless model of local heat transfer coefficients is proposed based on the packet renewal theory. The predictive and experimental values are well consistent with each other.

2. The local heat transfer model

2.1. The particle convection heat transfer model

Fig. 1 shows the heat transfer physical model between particle packets and tube surface in vibrated fluidized bed. Considering a micro-elemental volume of the particle packets, the assumptions are as following based on our previous study [17]

(1) Around the tube surface, there exists a thin gas film, and the thickness of gas film dependents on the vibration, the particle diameter and the local position on the tube surface. Unsteady state heat conduction through the gas film on the tube surface at first, and then heat transfer by unsteady state conduction from the gas film to the particle packets.
(2) The main factor affecting the contact time of particle packets is the vibration frequency. The gap width

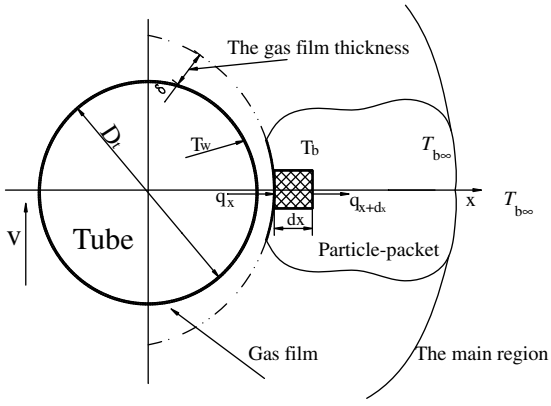

Fig. 1. Heat transfer model between particle packets and tube surface in the vibrated fluidized bed.

induced by vibration is included in the gas film thickness.

(3) The particle packets have the properties of the bed at critical fluidization.

(4) The temperature of the particle packets far from the tube surface remains unchanged at $T_{b\infty}$ during contacting heat transfer between the particle packets and the tube surface.

Based on the Fourier Law and the energy balance, the one-dimensional unsteady state conduction equation is

$$\begin{cases} \frac{\partial T_b}{\partial t} = \alpha \frac{\partial^2 T_b}{\partial x^2} \\ t = 0, T_b = T_\infty \\ x = 0, -k\left(\frac{\partial T_b}{\partial x}\right)_{x=0} = \frac{k_g}{\delta}(T_w - T_{b0}) \\ x \to D_t, T_b = T_\infty \end{cases} \tag{1}$$

The dimensionless variables are defined as

$$X^* = \frac{x}{D_t} = \text{dimensionless coordinate} \tag{2}$$

$$T_b^* = \frac{T_b - T_\infty}{T_w - T_\infty} = \text{dimensionless temperature} \tag{3}$$

$$Bi = \frac{hD_t}{k_e} = \frac{k_g D_t}{k_e \delta} = \text{Biot number} \tag{4}$$

$$t^* = \frac{\alpha t_e}{D_t^2} = \frac{k_e t_e}{\rho_e c_{pe} D_t^2} = \text{dimensionless time or } Fo \text{ number} \tag{5}$$

So Eq. (1) can be expressed by the following dimensionless form:

$$\begin{cases} \frac{\partial T_b^*}{\partial t^*} = \frac{\partial T_b^{2*}}{\partial x^{*2}} \\ t^* = 0, \quad T_b^* = 0 \\ X^* = 0, \quad \frac{\partial T_b^*}{\partial X^*} + Bi \cdot T_b^* = 0 \\ X^* = 1, \quad T_b^* = 0 \end{cases} \tag{6}$$

The solution of Eq. (6) is

$$T_b^* = \operatorname{erf}\frac{X^*}{2Fo^{1/2}} + \exp[Bi \cdot X^* + Bi^2 \cdot Fo] \cdot \operatorname{erfc}\left(\frac{X^*}{2Fo} + Bi \cdot Fo^{1/2}\right) \tag{7}$$

The heat flux, q, is given by

$$q = h_i(T_w - T_{b\infty}) \tag{8}$$

The heat flux depended on unsteady state conduction through a gas film is given by

$$q = \frac{k_g}{\delta}(T_w - T_{b0}) \tag{9}$$

Equating the two equations for the heat flux, and

$$h_i = \frac{k_g}{\delta}\frac{(T_w - T_{b0})}{(T_w - T_{b\infty})} = \frac{k_g}{\delta} \cdot T_b^*|_{X^*=0} \tag{10}$$

So the instantaneous heat transfer coefficient can be expressed by

$$h_i = \frac{k_g}{\delta}\exp(Bi^2 \cdot Fo) \cdot \operatorname{erfc}(Bi \cdot Fo^{1/2}) \tag{11}$$

The time average heat transfer coefficient can be obtained through integrated Eq. (11)

$$h_{pc} = \frac{\int_0^{Fo} \frac{k_g}{\delta}\exp(Bi^2 \cdot Fo) \cdot \operatorname{erfc}(Bi \cdot Fo^{1/2}) dFo}{\int_0^{Fo} dFo} \tag{12}$$

The mathematical model of the local particle convection heat transfer coefficients is as follow

$$h_{pc} = \frac{k_g}{\delta}\left\{\frac{1}{Bi^2 \cdot Fo}[\operatorname{erfc}(Bi \cdot Fo^{1/2}) \cdot \exp(Bi^2 \cdot Fo) - 1] + \frac{2}{Bi \cdot (\pi Fo)^{1/2}}\right\} \tag{13}$$

Eq. (13) is the dimensionless mathematical model of the local heat transfer coefficients between the vibrated fluidized beds and horizontal tubes. The two dimensionless variables can be obtained as follows:

(1) Biot number

$$Bi = \frac{hD_t}{k_e} = \frac{k_g/\delta}{k_e/D_t} \tag{14}$$

The physical meaning of Bi is contradistinctive thermal resistance. The two key parameters to be determined are the gas film thickness (δ) and the effective thermal conductivity (k_e).

(i) The gas film thickness, δ. The gas film thickness is very important parameter to affect the local heat transfer. The mechanical vibration imposed on fluidized bed can form crescent-gaps on the tube surface. So for the vibrated fluidized beds, the main influence factors on the gas film thickness include vibration, particle diameter and circumferential position of the tube surface. The thickness of the gas film can be calculated by

$$\delta = \frac{d_p}{a}\Gamma^b(1 + |\cos\theta|)^c \tag{15}$$

where the coefficients a, b and c in the equation above are shown in Table 1.

(ii) The effective thermal conductivity of the particle packets, k_e.

The effective thermal conductivity of the particle packets can be calculated as follow [19]

$$k_e = k_e^0 + 0.1 d_p u_{mf} \rho_g c_{pg} \tag{16}$$

Here u_{mf} is the critical fluidization velocity of the vibrated fluidized beds, it can be substitutes by u_{mfv}, and can be calculated by following equation [18]

$$\frac{u_{mfv}}{u_{mf}} = 1 - 0.04043 Ar^{0.1235}\left(\frac{H_0}{D}\right)^{-0.5613}\Gamma^{0.3653} \tag{17}$$

Table 1
Coefficients of gas film thickness model

	$\theta \leqslant 90°$, $\Gamma < 1$	$\theta \leqslant 90°$, $\Gamma \geqslant 1$	$\theta > 90°$, $\Gamma < 1$	$\theta > 90°$, $\Gamma \geqslant 1$
a	8.0	5.55	6.45	6.45
b	−0.3068	0.1646	−0.1252	0.1528
c	0.3576	0.1732	0.6292	0.7891

(2) *Fo* number

The dimensionless number *Fo* can be calculated by the following equation:

$$Fo = t^* = \frac{\alpha t_e}{D_t^2} = \frac{t_e}{D_t^2/\alpha} \tag{18}$$

Fo has the physical meaning of contradistinctive time. For the vibrated fluidized beds, the renewal frequency of particle packets on the tube surface is approximately equal to the vibration frequency. The particle surface contact time could be calculated by the following equation [20].

$$t_e = \frac{1}{f}\left(1 - \frac{1}{\pi}\right) \tag{19}$$

So Eq. (18) could be rewritten as

$$Fo = t^* = \frac{k_e t_e}{\rho_e c_{pe} D_t^2} = \frac{1}{f}\frac{k_e}{\rho_e c_{pe} D_t^2}\left(1 - \frac{1}{\pi}\right) \tag{20}$$

2.2. The gas convection heat transfer model

Baskakov and Suprun [21] predicted the gas convection heat transfer coefficients on immersed surface in a fluidized bed as

$$h_{gc} = \frac{k_g}{d_p} 0.0175 Ar^{0.46} Pr^{0.33} \left(\frac{u}{u_{mf}}\right)^{0.3} \tag{21}$$

The radiation's contribution to the heat transfer coefficients is considered important for the bed in which the temperature is higher than 800 °C, but can be neglected in the present studies since the experiment conditions are at low temperatures. So the total local heat transfer coefficients can be expressed by

$$h = (1 - f_0)(h_{pc} + h_{gc}) + f_0 h_g \tag{22}$$

Hence

$$h_{gc} = \frac{h - h_{pc} + f_0(h_{pc} - h_g)}{(1 - f_0)} \tag{23}$$

For large particles, $h_g = h_{gc}$, so

$$h_{gc} = h - (1 - f_0)h_{pc} \tag{24}$$

For the two-phase flow theory [22], the gas flow rate above that of the critical fluidization velocity goes into the bubble phase. So the bubble volume fraction can be calculated by the following equation.

$$u_b f_0 = u - u_{mf} \tag{25}$$

The average bubble velocity was given by Davidson and Harrison [22]

$$u_b = u - u_{mf} + 0.71\sqrt{gD_b} \tag{26}$$

In our study, the following correlation can predict the gas convection heat transfer coefficient:

$$h_{gc} = 0.01172 \frac{k_g}{d_p} Ar^{0.4850} \left(\frac{u}{u_{mfv}}\right)^{0.6235} \tag{27}$$

Here u_{mfv} is the critical fluidization velocity of the vibrated fluidized beds, and it can be obtained from Eq. (17).

3. The experiment apparatus and procedure

The schematic sketch of the experimental system is illustrated in Fig. 2. The two-dimensional fluidized bed with the cross-section of 240 mm × 80 mm and the height of 600 mm was made from Plexiglas plate to permit visual observation of the fluidization behavior. The gas distributor was a perforated metallic plate with the pore size of 2 mm and the opening fraction of 5%. A stainless steel screen with the mesh size of 0.15 mm was placed above on the distributor to gain more homogeneous distribution of the gas flow. The body of bed, supported by four springs, was vibrated in the vertical direction by means of an eccentric mechanism. The amplitude was adjusted by the variable eccentricity of the system and the frequency was controlled by means of a variable speed motor. The rate of fluidizing gas from a blower was measured by an orifice flow meter.

Fig. 3 shows the tube used for the experiments in this work to measure the local heat transfer coefficients. The tube, 25 mm in diameter and 80 mm in length, was made from Teflon cylinder imbedded with a small copper bar of 10 mm × 9 mm cross-section and 36 mm in length. The heater is 36 mm in length and 4 mm in diameter, and it was inserted into the hole drilled in the copper bar. The heater was centrally positioned in the copper bar. The tube was rigidly and horizontally assembled in the mid-plane of

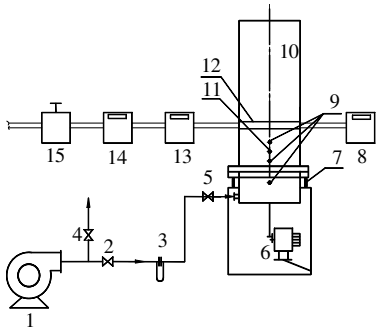

Fig. 2. Schematic sketch of the experimental system: 1, blower; 2, control valve; 3, orifice flow meter; 4, vent valve; 5, gas enter valve; 6, vibration electrometer; 7, spring; 8, digital thermometer; 9, pressure measure 10, fluidized bed; 11, temperature measure; 12, horizontal tube; 13, wattmeter; 14, manostat; 15, voltage regulator.

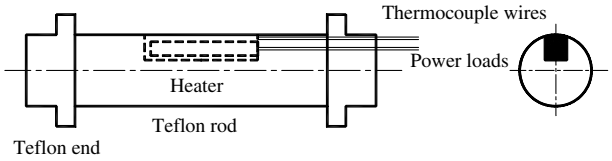

Fig. 3. The tube used for measuring the local heat transfer coefficients.

the bed, and its axial center being located 60 mm above the gas distributor. A copper–constantan thermocouple was welded at the center surface of the tube to measure temperature of the surface.

The temperatures of the bed and those of the tube surface were monitored with a digital thermometer. The power inputted to the heater was adjusted by a voltage regulator and measured with a wattmeter.

The bed vibrated under certain amplitude and frequency, and the power into the heater and the gas velocity were switched on. The experiment continued until the temperature of the tube surface reached a constant value. The local heat transfer coefficients is determined from the following relation

$$h_i = \frac{Q}{A_i(T_w - T_b)} \tag{28}$$

Here h_i is the local heat transfer coefficient, W m^{-2} K^{-1}. Q is the power inputted to the heater, J s^{-1}. A_i is the local area of the test tube, m^2. T_w and T_b are the temperatures of the tube surface and the bed, respectively, °C.

4. Results and discussion

4.1. Comparison of predictions with experimental data (D_t = 25 mm, H_0 = 95 mm)

Figs. 4–9 show the comparison of the variation between the model predictions and the experimental data with the average particle diameter ($\bar{d}_p = 1.83$ mm) under a certain

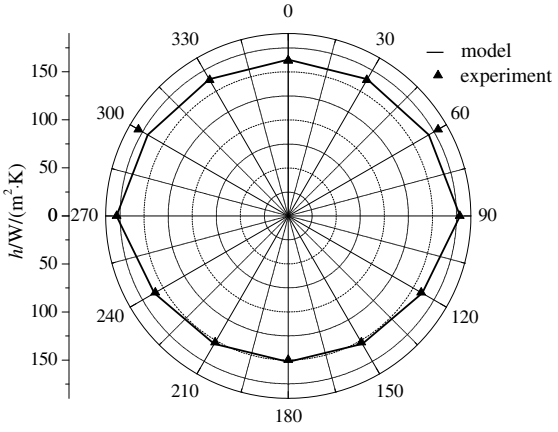

Fig. 4. Comparison of predictions with experimental measurement of the local heat transfer coefficients ($D_t = 25$ mm, $f = 6.67$ Hz, $N = 1$, $H_0 = 95$ mm).

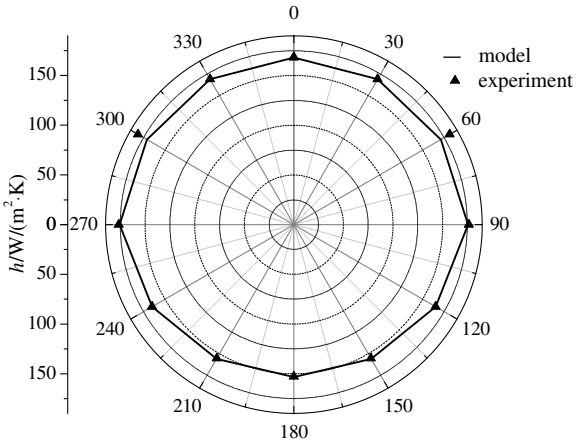

Fig. 5. Comparison of predictions with experimental measurement of the local heat transfer coefficients ($D_t = 25$ mm, $f = 11.17$ Hz, $N = 1$, $H_0 = 95$ mm).

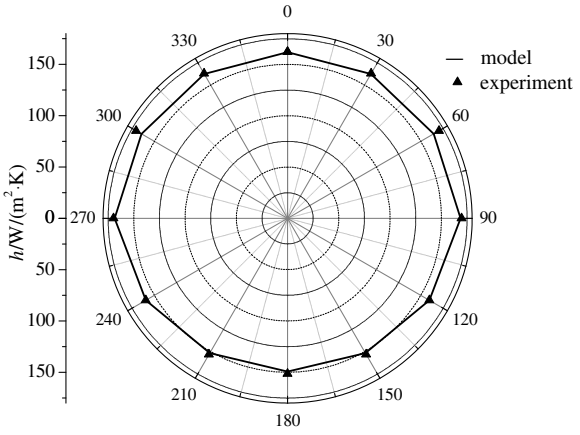

Fig. 6. Comparison of predictions with experimental measurement of the local heat transfer coefficients ($D_t = 25$ mm, $f = 15.83$ Hz, $N = 1$, $H_0 = 95$ mm).

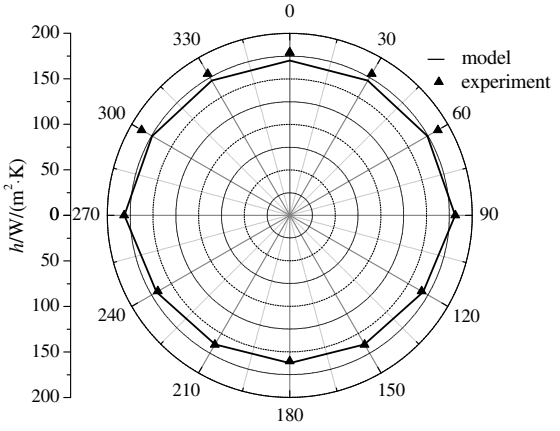

Fig. 7. Comparison of predictions with experimental measurement of the local heat transfer coefficients ($D_t = 25$ mm, $f = 6.67$ Hz, $N = 1.4$, $H_0 = 95$ mm).

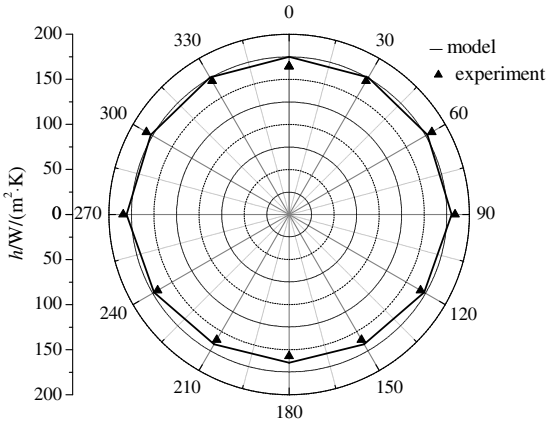

Fig. 8. Comparison of predictions with experimental measurement of the local heat transfer coefficients ($D_t = 25$ mm, $f = 11.17$ Hz, $N = 1.4$, $H_0 = 95$ mm).

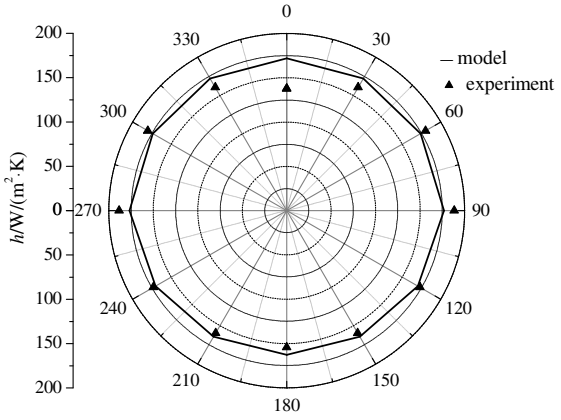

Fig. 9. Comparison of predictions with experimental measurement of the local heat transfer coefficients ($D_t = 25$ mm, $f = 15.83$ Hz, $N = 1.4$, $H_0 = 95$ mm).

vibration frequency and gas velocity. General agreements are found between the calculated values and the experimental data all around the tube. It is seen that the both show excellent agreement at $N = 1$ and all vibration frequency, the predicted values tend to be lower than experimental values measured on the leeward side of the tube at higher gas velocity ($N = 1.4$). Figs. 4–9 also tell that the local heat transfer coefficients on the leeward side of the tube were higher than the values on the windward side. It is due to the differences of the hydrodynamic behavior of the particles on the surface of the horizontal tube, and the particle-free gaps on the windward side of the tube can be observed.

4.2. Comparison of predictions with experimental data at D_t = 32 mm

Fig. 10 shows the comparison of the variation between the model predictions and the experimental data

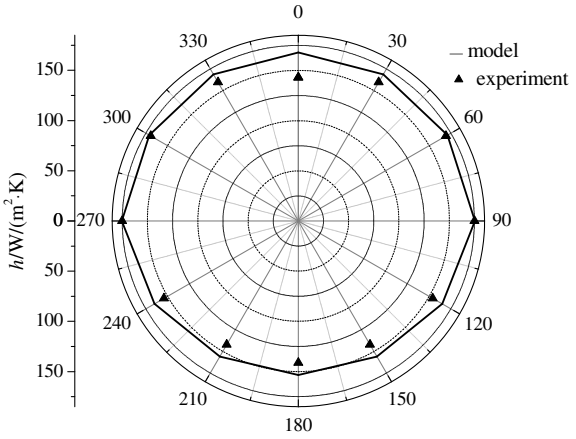

Fig. 10. Comparison of predictions with experimental measurement of the local heat transfer coefficients ($D_t = 32$ mm, $f = 11.17$ Hz, $N = 1$, $H_0 = 95$ mm).

($D_t = 32$ mm) at the same vibration frequency ($f = 11.17$ Hz) and fluidization number ($N = 1$). It is seen that the predicted values tend to be lower than experimental values measured. It may be due to the fact that the model in this study does not consider the influence of the tube diameter on the local heat transfer coefficients. The hydrodynamic behavior of the particles on different horizontal tubes is difference. So there are some differences in the distribution of the local heat transfer coefficients between horizontal tubes with different diameter.

4.3. Comparison of predictions with experimental data at H_0 = 130 mm

Fig. 11 shows the comparison of the variation between the model predictions and the experimental data with static bed height ($H_0 = 130$ mm) under vibration frequency ($f = 11.17$ Hz) and fluidization number ($N = 1$). It is seen that the predicted values are little lower than experimental measured values. It may be due to the fact that the model

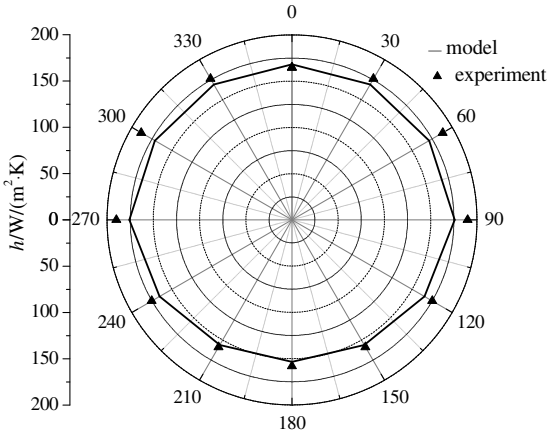

Fig. 11. Comparison of prediction with experimental measurement of the local heat transfer coefficients ($D_t = 25$ mm, $f = 11.17$ Hz, $N = 1$, $H_0 = 130$ mm).

of this study only considered that the local heat transfer coefficients decrease while the bed height increasing, that is, the vibration is dissipated along with the bed height, and the higher the bed height is, the weaker heat transfer influenced by the vibration. At the same time the fluidization quality is worse as the bed height increase. The influence of bed height on the local heat transfer coefficients from the literature is conflict. But from our experimental data, the influence of bed height on the local heat transfer coefficients is different on the circumferential position of the tube surface. There are certain differences between the prediction values and the experimental measures, and the position of the maximum error is 60°, but the error is generally less than 10%. So the model is able to predict the local heat transfer coefficients with different bed height.

4.4. Comparison with other's published data

The comparison between the predicted values from the correlations proposed by this study and Al-Busoul's [13] with the experimental values is shown in Fig. 12. Al-Busoul's curve was obtained by their model under the same conditions of our study except $f = 0$. There is great difference in the distribution of the local heat transfer coefficients between our results and Al-Busoul's. The model of Al-Busoul's is mainly fit for small particles. In this study the existence of vibrating can break the bubbles more efficiently, and enhance the contact of the gas and the particles, so the distribution of the local heat transfer coefficients is more homogeneous. The model of this study seems better to predict local heat transfer coefficients between vibrated fluidized beds and immersed horizontal tubes with large particles.

4.5. Error analysis

The comparison between the predicted local heat transfer coefficients from the correlations proposed by this study and the experimental values is shown in Fig. 13 (130 data points). It is seen that the model is able to predict the variation of the local heat transfer coefficients at circumferential position reasonably well, and the maximum error does not exceed 15%, the root-mean-square deviations of the predicted local heat transfer coefficients and the experimental values is 5.64%. Thus the model proposed by this study can be used to predict the local heat transfer coefficients for horizontal tube immersed in vibrated fluidized beds with large particles ($\bar{d}_p > 1$ mm).

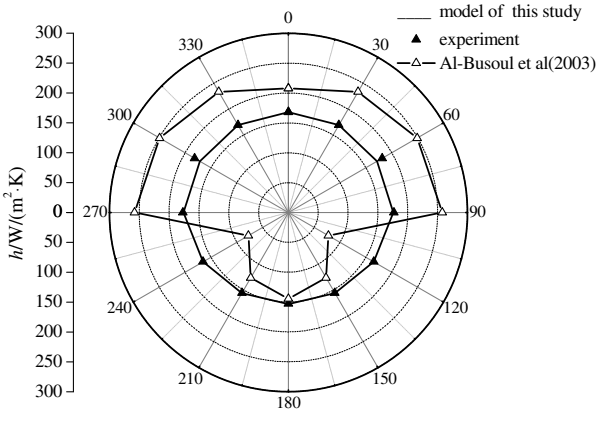

Fig. 12. Comparison of predictions and experimental measurement of the local heat transfer coefficients in this study with Al-Busoul's.

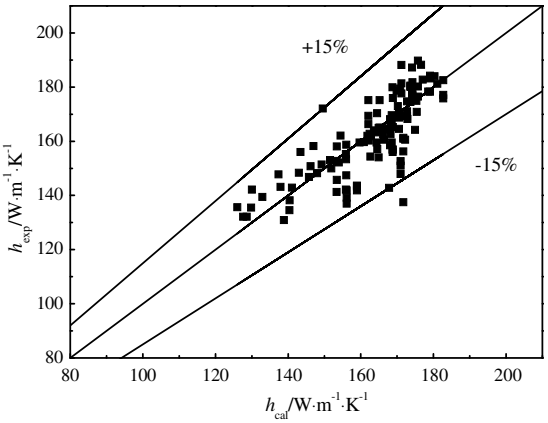

Fig. 13. Comparison of predictions with experimental measurement of the local heat transfer coefficients.

5. Conclusions

In this study a mathematical model and the experimental data of the local heat transfer coefficients between vibrated fluidized beds and immersed horizontal tubes have been presented. Based on this study, the following conclusions can be drawn:

(1) A dimensionless mathematical model including the particle convection heat transfer coefficients model and the gas convection heat transfer coefficients model are proposed to predict the local heat transfer coefficients between the vibrated fluidized beds and immersed horizontal tubes.
(2) The renewal frequency of particle packets on the tube surface is equal to the vibration frequency. The gas film thickness around the tube surface depends on the vibration, the particle diameter and the local position on the tube surface. The empirical correlation is developed to calculate the gas film thickness, and the correlation can predict the gas film thickness well.
(3) The local heat transfer coefficients between the vibrated fluidized beds and tube surface are different from conventional fluidized bed. The values on the leeward side of the tube are higher than the windward side.
(4) The values of theoretical prediction are in good agreement with the experimental data, so the model is able to predict the local heat transfer coefficients between vibrated fluidized beds and immersed horizontal tubes reasonably well.

Acknowledgements

The authors wish to acknowledge the Nature Science Foundation of PanZhihua University (B2006-05), for financial support, and the experimental help of Qingxia Shi and Bingshi Yang of Sichuan University.

References

[1] J.F. Davidson, D. Harrison, Fluidization, Academic Press, London and New York, 1971.
[2] N.S. Grewal, J. Menart, Heat transfer to horizontal tubes immersed in a fluidized bed combustor, Powder Technology 52 (2) (1987) 149–159.
[3] D. Kunii, O. Levenspiel, Fluidization Engineering, John Wiley and Sons, Inc., New York, 1969.
[4] X.J. Zhu, Q. Lv, S.C. Ye, Experimental study on the drying of paste materials in a vibrated fluidized bed with inert particles, Journal of Chemical Industry and Engineering 58 (7) (2007) 1663–1669.
[5] W.M. Dow, M. Jakob, Heat transfer between a vertical tube and a fluidized air–solid mixture, Chemical Engineering Progress 47 (2) (1951) 637.
[6] C. Van Heerden, P. Nobel, D.W. Van Krevelen, Mechanism of heat transfer in fluidized beds, Industrial and Engineering Chemistry 45 (1953) 1237–1242.
[7] E.N. Ziegler, W.T. Brazelton, Mechanism of heat transfer to fixed surfaces in fluidized beds, Industrial and Engineering Chemistry Fundamentals 3 (1964) 94–98.
[8] H.S. Mickley, D.F. Fairbanks, Mechanism of heat transfer to fluidized beds, AIChE Journal 1 (1955) 374–384.
[9] D.H.Y. Lei, An experimental study of radiative and total heat transfer between a high temperature fluidized bed and an array of immersed tubes, Ph.D. Thesis, Oregon State University, 1988.
[10] R. Chandran, J.C. Chen, A heat transfer model for tubes immersed in gas fluidized beds, AIChE Journal 31 (2) (1985) 244–252.
[11] J.S. Botterill, J.R. Williams, The mechanism of heat transfer model to gas fluidized beds, Transactions of the Institution of Chemical Engineering 41 (1963) 217–230.
[12] L. Wang, P. Wu, X.Z. Ni, Surface-particle-emulsion model of heat transfer between a fluidized bed and an immersed surface, Powder Technology 149 (2005) 127–138.
[13] M.A. AL-Busoul, S.K. Abu-Ein, Local heat transfer coefficient around a horizontal heated tube immersed in a gas fluidized bed, Heat and Mass Transfer 39 (4) (2003) 355–358.
[14] S.R. Sunderesan, N.N. Clark, Local heat transfer coefficients on the circumference of a tube in a gas fluidized bed, International Journal of Multiphase Flow 21 (6) (1995) 1003–1024.
[15] N.S. Grewal, A generalized correlation for heat transfer between a gas–solid fluidized bed of small particles and an immersed staggered array of horizontal tubes, Powder Technology 30 (2) (1981) 145–154.
[16] C.I. Anekwe, Heat transfer in horizontal tubes immersed in fluidized beds, Ph.D. Thesis, West Virginia University, 1982.
[17] S.C. Ye, Heat transfer between immersed horizontal tubes and aerates vibrated fluidized beds, Ph.D. Thesis, Sichuan University, 2000.
[18] X.J. Zhu, Q. Lv, S.C. Ye, Theoretical prediction and experimental investigation on the critical fluidization velocity of vibrated fluidized bed, Journal of Chemical Engineering of Chinese Universities 21 (1) (2007) 59–63.
[19] Z.H. Lin, D.S. Wei, E.K. An, Circulating Fluidized Bed Boilers, Chemical Industry Press, Beijing, 2004.
[20] K. Malhotro, A.S. Mujumdar, Immersed surface heat transfer in a vibrated fluidized bed, Industrial and Engineering Chemistry Research 26 (10) (1987) 1983–1992.
[21] A.P. Baskakov, V.M. Suprun, Determination of the convective component of the heat transfer coefficient to a gas in a fluidized bed, International Chemical Engineering 12 (2) (1972) 324–326.
[22] Y. Jin, J.X. Zhu, Z.W. Wang, et al., Fluidization Engineering Principles, Tsinghua University Press, Beijing, 2001.